Available online at www.sciencedirect.com
ScienceDirect
New Astronomy Reviews 50 (2006) 977–983
New Astronomy Reviews
www.elsevier.com/locate/newastrev

The Cosmic Foreground Explorer (COFE): A balloon-borne microwave polarimeter to characterize polarized foregrounds

Rodrigo Leonardi [a,b,*], Brian Williams [a], Marco Bersanelli [c], Ivan Ferreira [b], Philip M. Lubin [a], Peter R. Meinhold [a], Hugh O'Neill [a], Nathan C. Stebor [a], Fabrizio Villa [d], Thyrso Villela [b], Carlos A. Wuensche [b]

[a] *Physics Department, University of California, Santa Barbara, CA 93106, United States*
[b] *Instituto Nacional de Pesquisas Espaciais, Divisão de Astrofísica, Caixa Postal 515, 12227-010, São José dos Campos, SP, Brazil*
[c] *Dipartimento di Fisica, Università degli Studi di Milano, Via Celoria 16, 20133 Milan, Italy*
[d] *INAF - IASF Bologna, Via P. Gobetti, 101, 40129 Bologna, Italy*

Available online 13 November 2006

Abstract

The COsmic Foreground Explorer (COFE) is a balloon-borne microwave polarimeter designed to measure the low-frequency and low-ℓ characteristics of dominant diffuse polarized foregrounds. Short duration balloon flights from the Northern and Southern Hemispheres will allow the telescope to cover up to 80% of the sky with an expected sensitivity per pixel better than 100 $\mu K/deg^2$ from 10 GHz to 20 GHz. This is an important effort toward characterizing the polarized foregrounds for future CMB experiments, in particular the ones that aim to detect primordial gravity wave signatures in the CMB polarization angular power spectrum.

Keywords: Cosmology: observations; Cosmic microwave background; Polarization foregrounds

Contents

1. Introduction . . . 978
2. Science . . . 978
3. Instrumentation . . . 978
   3.1. Telescope . . . 978
   3.2. Polarization modulator . . . 979
   3.3. Receiver . . . 979
   3.4. Data acquisition/demodulation . . . 980
   3.5. Ground-based B-machine prototype . . . 980
4. Performance . . . 981
   4.1. Receiver bands and expected receiver sensitivity . . . 981
   4.2. Scan strategy, sky coverage and expected map sensitivity . . . 982
5. Conclusion . . . 982
   Acknowledgements . . . 983
   References . . . 983

* Corresponding author. Address: Physics Department, University of California, Santa Barbara, CA 93106, United States.
E-mail address: rodrigo@deepspace.ucsb.edu (R. Leonardi).

1387-6473/$ - see front matter
doi:10.1016/j.newar.2006.09.004

1. Introduction

Measurement of polarization anisotropies in the Cosmic Microwave Background (CMB) is one of the great challenges in cosmology today. Very sensitive measurements of these anisotropies, particularly at large angular scales, will provide unique constraints on the influence of gravitational waves on the production of structure in the very early Universe and information on the epoch of reionization.

Several experiments are running or in the planning stages, and long term development for a future space mission attacking CMB polarization is underway. To date, nearly all of the effort has been directed towards maximizing the number of detectors in the focal plane to achieve the required sensitivity. Relatively little work is going into sub-orbital efforts to constrain polarization fluctuations at the largest angular scales, those most interesting for their impact on understanding the inflationary epoch and ionization history of the universe. This is primarily because of an unproven perception that very low multipoles will not be accessible to any but space-based missions. Indeed, large scale polarization has been searched for with ground based experiments over the last 30 years. The COsmic Foreground Explorer (COFE) is a balloon-borne instrument to measure the low frequency and low-ℓ characteristics of some dominant polarized foregrounds. Good understanding of these foregrounds is critical both for interpreting recent results, e.g. Spergel et al. (2006), and for appropriately planning future CMB missions. The experiment also explores low-ℓ limits to CMB polarization measurements at moderate frequencies from non-space based platforms. We believe that balloon and ground-based measurements to characterize in detail the polarized microwave sky are essential to prepare a future space mission dedicated to CMB B-modes.

2. Science

The CMB radiation field is an observable that provides direct information from the early Universe. The temperature and polarization characteristics of this field impose constraints on cosmological scenarios relevant to understand the origin and the structure of the Universe. Accurate measurements of the CMB are vital to improve our understanding about geometry, mass-energy composition, and reionization of the Universe. Ultimately, the CMB could also provide indirect detection of a stochastic gravitational background and information from the inflationary epoch itself. Having this big picture in mind, several CMB experiments are now trying to constrain the tensor-to-scalar ratio value and to detect the signature.

Among all practical limitations to primordial tensor amplitude detection, contamination due diffuse microwave foreground polarized emission is certainly the fundamental one. This emission presents spatial and frequency variations that are not well known, and the residuals from foreground subtraction are restricting our knowledge of CMB polarization. This is particularly true for future B-mode experiments that will benefit if accurate determinations of spatial and spectral characteristics of polarized foreground are made. For this reason, multifrequency measurements of the polarized foregrounds in the microwaves is now recognized as a key objective within the CMB community.

At low frequencies, foregrounds include synchrotron, free-free, and possible spinning dust emission. Synchrotron dominates the low frequency range of the microwave sky. Its emission is caused by relativistic charged particles interacting with the Galactic magnetic field and can be highly polarized. Synchrotron measurements provide better understanding of the Galactic magnetic field structure and the density of relativistic electrons across the Galaxy. Free-free emission becomes more important in the microwave intermediate frequency range, and it is due to electron-ion scattering. Free-free is expected to be unpolarized but this might not be true at the edges of HII clouds. Electrical dipole emission from spinning dust has also been suggested by recent observations at low microwave frequencies, e.g. Finkbeiner et al. (2004).

COFE is a balloon-borne microwave polarimeter to measure spatial and low-frequency characteristics of diffuse polarized foregrounds. This is an important effort toward characterizing the polarized foregrounds for future CMB experiments, in particular the ones that aim to detect primordial gravitational wave signatures in the CMB polarization angular power spectrum.

3. Instrumentation

3.1. Telescope

A modified BEAST telescope design is the basis for the COFE optics (Childers et al., 2005; Figueiredo

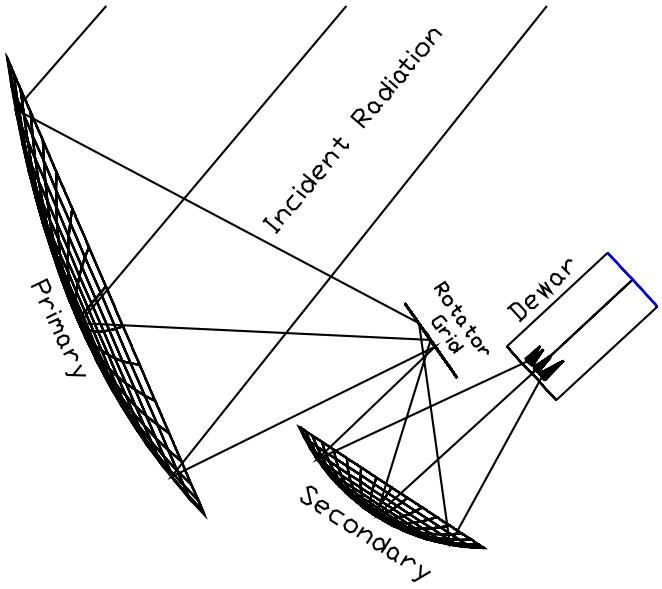

Fig. 1. Optical schematic for COFE and B-machine prototype telescopes, an off-axis Gregorian configuration optimized for minimal cross-polarization contamination. A 2.2 m parabolic reflector primary, a 0.9 m ellipsoidal secondary, and a 0.3 m rotator grid are shown.

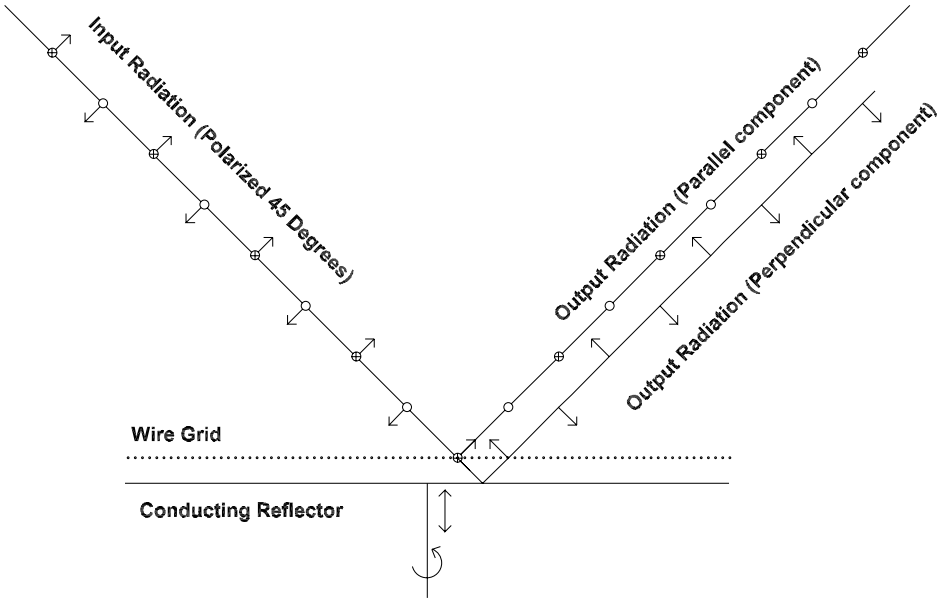

Fig. 2. Schematic of the polarization modulator. The input wave is decomposed into its two linear polarization states, parallel and perpendicular to the wires (represented by dots just above the conducting reflector). The perpendicular component is phase shifted from the extra path length. When added back to the parallel component, the plane of polarization of the input wave is rotated.

et al., 2005; Meinhold et al., 2005; Mejía et al., 2005; O'Dwyer et al., 2005). It consists of an off-axis Gregorian configuration obeying the Dragone–Mizuguchi condition (Dragone, 1978; Mizuguchi et al., 1978). The telescope is optimized for minimal cross-polarization contamination and maximum focal plane area. The primary reflector is a 2.2 m off-axis parabolic reflector. The incoming radiation is reflected off of the primary reflector towards a polarization modulating wave plate then to the secondary reflector. The 0.9 m ellipsoidal secondary reflects the incoming radiation toward the array of scalar feed horns that couple the radiation to an array of cryogenic low noise amplifiers. The telescope will be mounted in a gondola that has been simplified from a standard balloon-borne design due to the very light carbon fiber optical elements. A schematic of the optics is shown in Fig. 1.

3.2. Polarization modulator

A modified COFE will employ a low-loss reflective polarization modulator for measuring both Q and U simultaneously. It consists of a linear polarizing wire grid mounted in front of a reflecting plate. The wire grid decomposes the input wave into components, parallel and perpendicular to the wires, reflecting the parallel component with low loss. The perpendicular component passes through the wire grid and reflects off the back short, passes through the grid again and recombines with the parallel component. The distance between the plate and the grid introduces a phase shift between the two components, effectively rotating the plane of polarization of the input wave. A schematic of the polarization modulator is shown in Fig. 2. Rotating the grid chops between the two polarization states four times per revolution as shown in Fig. 3.

Tests of this modulator were performed at 41.5 GHz, using a 70 cm telescope. We measured beam patterns for the rotated polarization states and integrated for extended periods on the sky in Santa Barbara, CA. We were able to determine a $1/f$ knee lower than 50 mHz and very stable long term offsets. We also demodulated sky data to the two different states and calculated the correct combined sensitivity, as seen in Fig. 4.

The polarization modulator has a broad bandwidth. We achieved 22 dB isolation at 20% bandwidth. The radiometric loss of the elements in the modulator can easily be made very low (of order 0.1–1%) up to relatively high frequencies. The system works for a very wide range of frequency bands.

3.3. Receiver

COFE will use InP MMIC[1] amplifiers integrated into simple total power receivers. All of the RF gain will be integrated into a small compact module inside the vacuum chamber. The module will contain 3 to 4 amplifiers (~75 dB of gain), band pass filter, cryogenic detector diode, and an audio amplifier. The module avoids the need for cryo/vacuum waveguide feedthrus on the dewar simplifying the overall design. The audio amplifiers will be within the cryostat vacuum vessel for simplicity and noise reasons, but will be at ambient temperatures. COFE has a modest

[1] Indium Phosphide Monolithic Microwave Integrated Circuit.

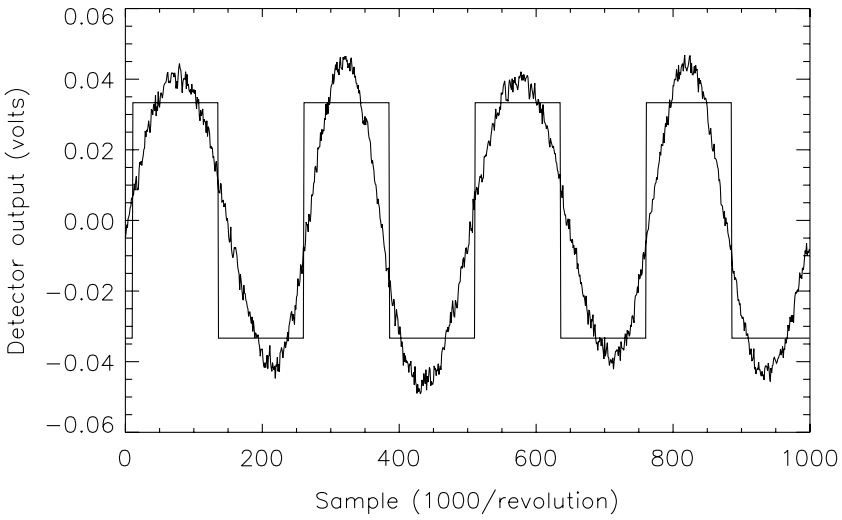

Fig. 3. Sample signal from a polarized thermal source. A single revolution of the modulator is shown, along with the reference signal to be used for demodulation. Commutating using this signal yields Q, for instance, while demodulating with a reference phase shifted by $\pi/4$ gives U.

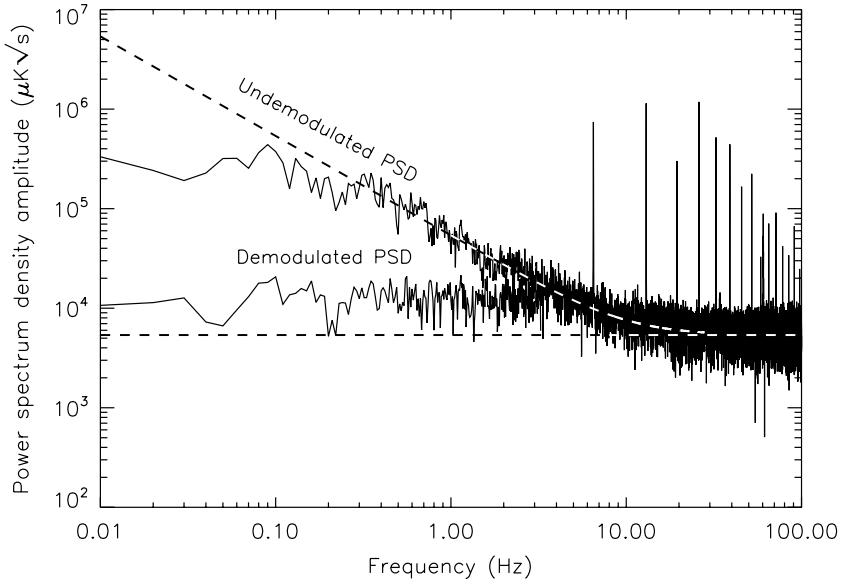

Fig. 4. Sample data from our room temperature radiometer viewing the sky at 41.5 GHz. The undemodulated PSD displays the $1/f$ knee of the HEMT radiometer of 10 Hz and a white noise of 5.4 mK$\sqrt{s}$. The demodulated data have no visible $1/f$ and a white noise level consistent with expectation.

number of feeds required, and no orthomode transducers or hybrid tees, so the passive components are minimal. A schematic of the receiver is shown in Fig. 5.

3.4. Data acquisition/demodulation

Data acquisition will use the same technique we have been using in our test system, namely synchronous sampling of analog integrators. We oversample the data by a large factor and perform the demodulation of Q and U Stokes parameters (and other modes for systematic error analysis) in software. This yields the most information and allows a variety of post-flight tests including null signal analysis and analysis of the DC or total power components (contaminated with $1/f$, but still useful for systematic tests).

3.5. Ground-based B-machine prototype

A prototype polarimeter for a B-mode project, named B-machine, is being deployed at the WMRS[2] Barcroft facility, CA (118°14′ W longitude, 37°35′ N latitude, 3800 m altitude). The WMRS facility is an excellent site for microwave observation because of a cold microwave zenith temperature, low precipitable water vapor, and a high percentage of clear days (Marvil et al., 2006). Many

[2] White Mountain Research Station.

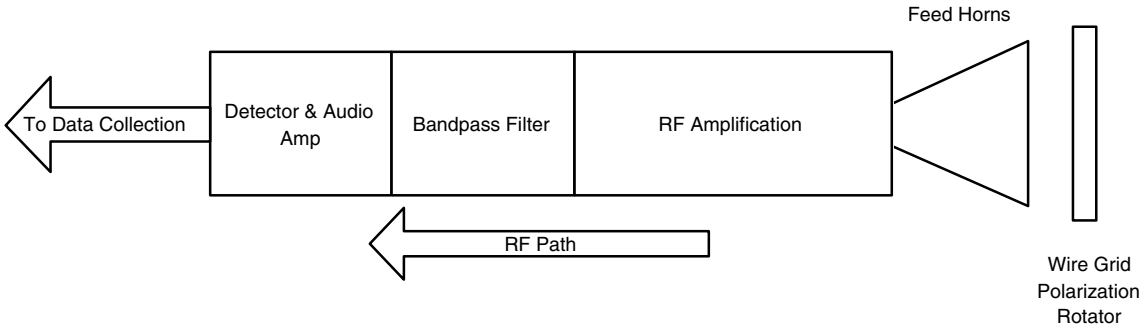

Fig. 5. Radiometer layout for COFE.

of the components that will be used by the B-machine prototype are useful for COFE as well. For example, the prototype will allow systematic checks of the polarization modulator, and COFE scan strategy. The B-machine prototype will be able to yield some basic higher multipole results on the foregrounds as well as the polarization signature and establish a data analysis pipeline.

The prototype possesses telescope and detector technology identical to COFE. It has 2 Ka-band and 6 Q-band channels centered at 31 and 41.5 GHz with FWHM resolution of 28′ and 20′ respectively. The receiver has been previously used in anisotropy measurements (Childers et al., 2005). The telescope runs at constant elevation while continuously scanning the sky in azimuth. A photograph of B-machine prototype is shown in Fig. 6.

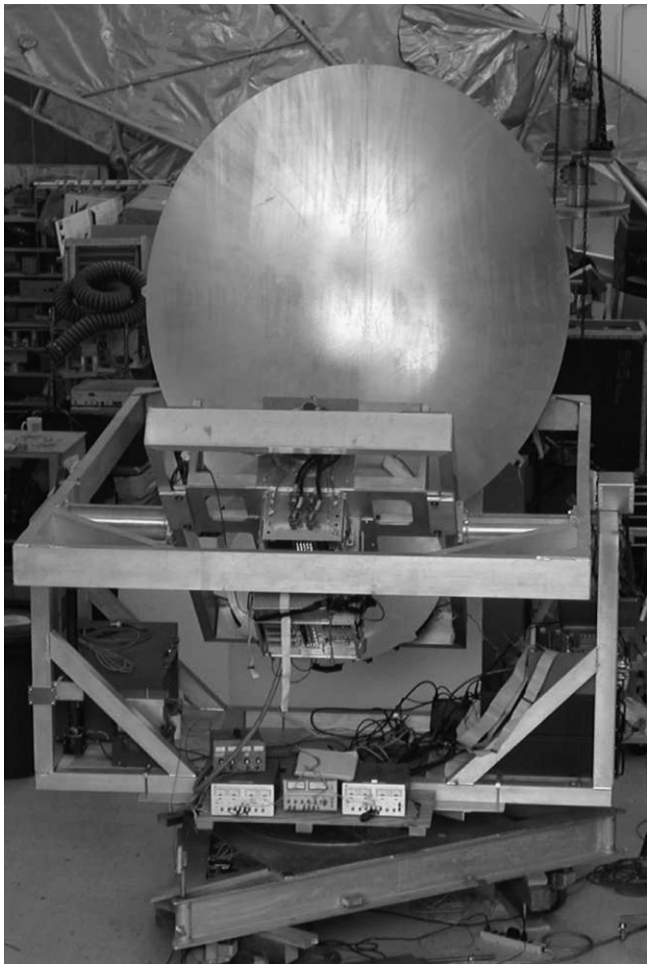

Fig. 6. Picture of prototype telescope to be deployed at WMRS.

4. Performance

For any sub-orbital CMB experiment, minimizing atmospheric contamination is important. For the COFE bands, total atmospheric emission at our target altitude of 35 km is less than 1 mK. Common broad band bolometric atmospheric antenna temperature contributions at balloon altitudes are several hundred mK or more. Since the effective CMB antenna temperature drops with frequency, our effective atmospheric signal is approximately 1000 times less than for a bolometric balloon-borne system. Hence low-ℓ information from a balloon-borne system is very clean by comparison. Fig. 7 shows the atmosphere and predicted foreground emission over a range of frequencies interesting for CMB work (the foreground prediction is calculated from Bennett et al., 2003).

4.1. Receiver bands and expected receiver sensitivity

Receiver sensitivity can be estimated according to the radiometer equation

$$\sigma_T = K\left(\frac{T_{\rm sys} + T_{\rm sky}}{\sqrt{\Delta\nu \cdot \tau}}\right), \tag{1}$$

where σ_T is the root-mean-square noise, $T_{\rm sys}$ is the system noise temperature, $T_{\rm sky}$ is the sky antenna temperature, $\Delta\nu$ is the bandwidth, τ is the integration time, and K is the sensitivity constant of the receiver.

For COFE and B-machine prototype the sensitivity constant of each receiver is $K = \frac{\pi}{2}$. The signal is sine wave modulated, reducing the sensitivity by a factor of $\frac{\pi}{2}$ as compared with a standard Dicke receiver, with an addition factor of $\frac{1}{2}$ from the standard definition for Q and U in the Rayleigh–Jeans regime of the CMB spectrum. Table 1 shows our estimation of the sensitivity of each receiver.

By increasing the number of receivers, future ground-based or balloon-borne experiments can significantly

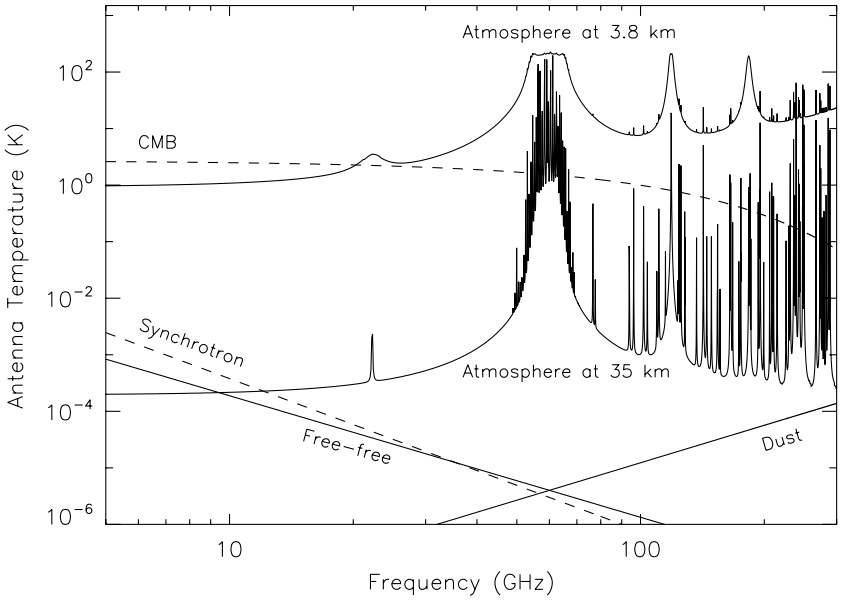

Fig. 7. Atmosphere, CMB, and predicted foreground emission from 5 to 300 GHz. COFE bands run from 10 to 20 GHz. The zenith atmosphere emission is shown at 3.8 and 35 km. The atmospheric emission and lines are mainly due to H_2O, O_2, and O_3. For the target altitude of 35 km, we expect well under 1 mK total emission from the atmosphere. Foreground spectral index β for free-free, synchrotron, and dust were assumed, respectively, as −2.15, −2.7, and 2.2.

Table 1
Instrument parameters

	COFE			B-machine	
Central frequency (GHz)	10	15	20	31	41.5
FWHM beam (arcmin)	83	55	42	28	20
T_{sys} (K)	8	10	12	25	27
T_{sky} (K) at target altitude[a]	2.5	2.4	2.3	6.4	13.0
Bandwidth (GHz)	4	4	5	10	7
Number of receivers	3	6	10	2	6
Sensitivity per receiver ($\mu K\sqrt{s}$)	261	308	318	493	751
Aggregate sensitivity ($\mu K\sqrt{s}$)	151	126	100	348	307

[a] For COFE and B-machine (ground-based), we compute expected T_{sky} antenna temperature at target altitude of 35 km and 3.8 km, respectively.

improve aggregate sensitivity. For instance, 30 detectors could reach 61 $\mu K\sqrt{s}$ and 107 $\mu K\sqrt{s}$ at 30 and 40 GHz, respectively.

4.2. Scan strategy, sky coverage and expected map sensitivity

COFE uses a simple scan strategy to cover the largest available sky area in each flight. The telescope will be pointed nominally 45° from the horizon to minimize ground and balloon pickup, and the gondola will rotate constantly at approximately 1/2 rpm. Data acquisition sample rate will be synchronized with the polarization rotator (at ~30 Hz). For instance, using this strategy, a 24 hour flight from Fort Sumner, NM, allows to cover 59% of the sky area with a median aggregate pixel sensitivity of 92 $\mu K/deg^2$, 77 $\mu K/deg^2$, and 61 $\mu K/deg^2$ at 10 GHz, 15 GHz, and 20 GHz respectively. COFE will acquire data from nearly all of the sky (~93%). This will be achieved in a set of 12 and/or 24 h flights from the Northern and Southern Hemispheres. Fig. 8 provides estimates for sensitivity per square degree pixel over the whole sky for our flight plans. Fig. 9 illustrates the expected sky coverage.

The B-machine prototype focuses on higher multipoles but uses a similar scanning strategy from the ground. For a conservative 60 day observing campaign at WMRS, we expect to cover 56% of the sky with an median aggregate sensitivity of 27 $\mu K/deg^2$, and 23 $\mu K/deg^2$ at 31 GHz and 41.5 GHz, respectively.

5. Conclusion

Over the next few years we will field a balloon-borne telescope to map more than 90% of the sky. Both polarization anisotropy and polarized foregrounds will be measured over several bands. This is an important effort toward characterizing the polarized foregrounds for future CMB experiments.

In addition to foreground detection, COFE will better characterize the polarization modulation capability for measuring Q and U simultaneously. As discussed earlier, a large scale ground-based campaign will capitalize on the technology that has been developed by COFE and B-machine prototype.

It is clear that our current understanding of the polarization foregrounds limits our ability to make accurate observations of the B-mode signature. COFE will lessen the effect that incomplete models of foregrounds will have on future experiments.

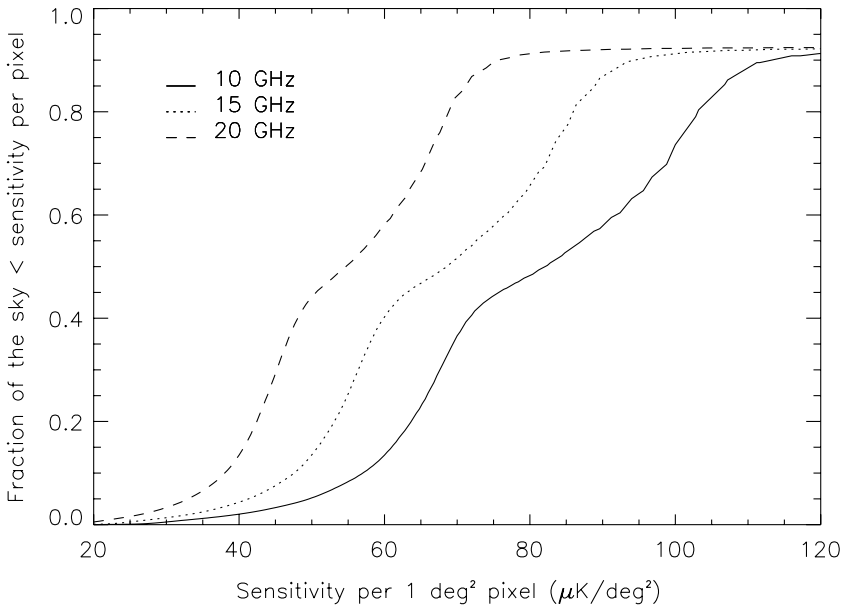

Fig. 8. Integrated histogram of anticipated aggregate sensitivity per 1 deg^2 pixel assuming a 24 h flight from the Northern Hemisphere (Fort Sumner, NM) and a 24 h flight from the Southern Hemisphere (Alice Springs, Australia). For each COFE band, we plot the fraction of the entire sky measured with better than a given aggregate sensitivity. The change of the curves slope is due to the fact that 35% of the sky can be observed from both hemispheres using COFE scan strategy.

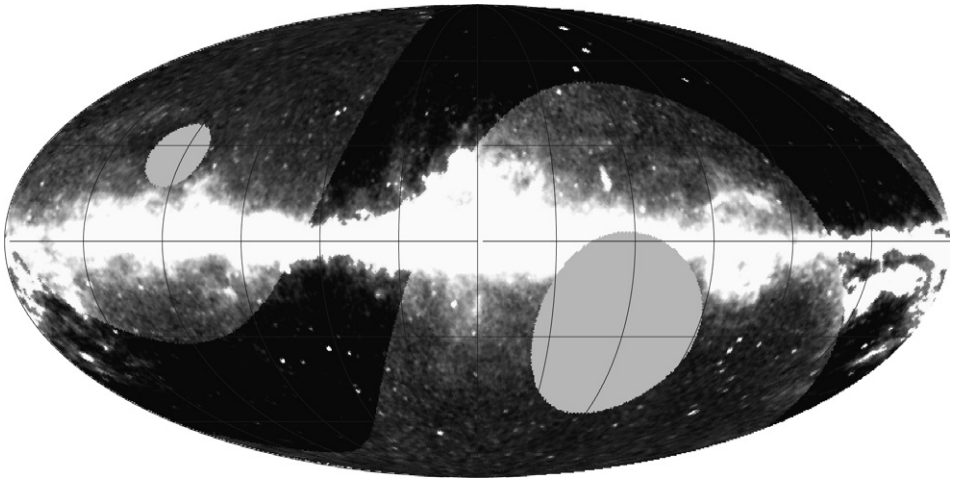

Fig. 9. Sky coverage for COFE assuming a 24 h flight from the Northern Hemisphere (Fort Sumner, NM) and a 24 h flight from the Southern Hemisphere (Alice Springs, Australia). The region observed contains nearly the entire sky (93%). The darker strip shows the overlap between the two observations. For illustration purposes, we show the diffuse Galactic structure obtained adding synchrotron, free-free and dust maps at 23 GHz (Bennett et al., 2003).

Acknowledgements

We acknowledge support from the National Aeronautics and Space Administration (NASA), and the California Space Institute (CalSpace). T.V. and C.A.W. acknowledge CNPq Grants 305219/2004-9 and 307433/2004-8, respectively. Some of the results have been derived using the HEALPix[3] (Górski et al., 2005) package. We would like to thank John Perlin for putting up with our discussions and cleaning up our language.

[3] http://healpix.jpl.nasa.gov.

References

Bennett, C.L. et al., 2003. ApJS 148, 97.
Childers, J. et al., 2005. ApJS 158, 124.
Dragone, C., 1978. The Bell System Technical Journal 57 (7), 266.
Figueiredo, N. et al., 2005. ApJS 158, 118.
Finkbeiner, D.P. et al., 2004. ApJ 617, 350.
Górski, K.M. et al., 2005. ApJ 622, 759.
Marvil, J. et al., 2006. New Astronomy 11, 218.
Meinhold, P.R. et al., 2005. ApJS 158, 101.
Mejía, J. et al., 2005. ApJS 158, 109.
Mizuguchi, Y., Akagawa, M., Yokoi, H., 1978. Electronics and Communications In Japan 61, 58.
O'Dwyer, I.J. et al., 2005. ApJS 158, 93.
Spergel, D.N., et al., 2006. Available from: <astro-ph/0603449>.